CO_2 Reduction Hot Paper

Zitierweise: *Angew. Chem. Int. Ed.* **2023,** *62,* e202300226
Internationale Ausgabe: doi.org/10.1002/anie.202300226
Deutsche Ausgabe: doi.org/10.1002/ange.202300226

Achieving High Single-Pass Carbon Conversion Efficiencies in Durable CO_2 Electroreduction in Strong Acids via Electrode Structure Engineering

*Le Li, Zhaoyang Liu, Xiaohan Yu, and Miao Zhong**

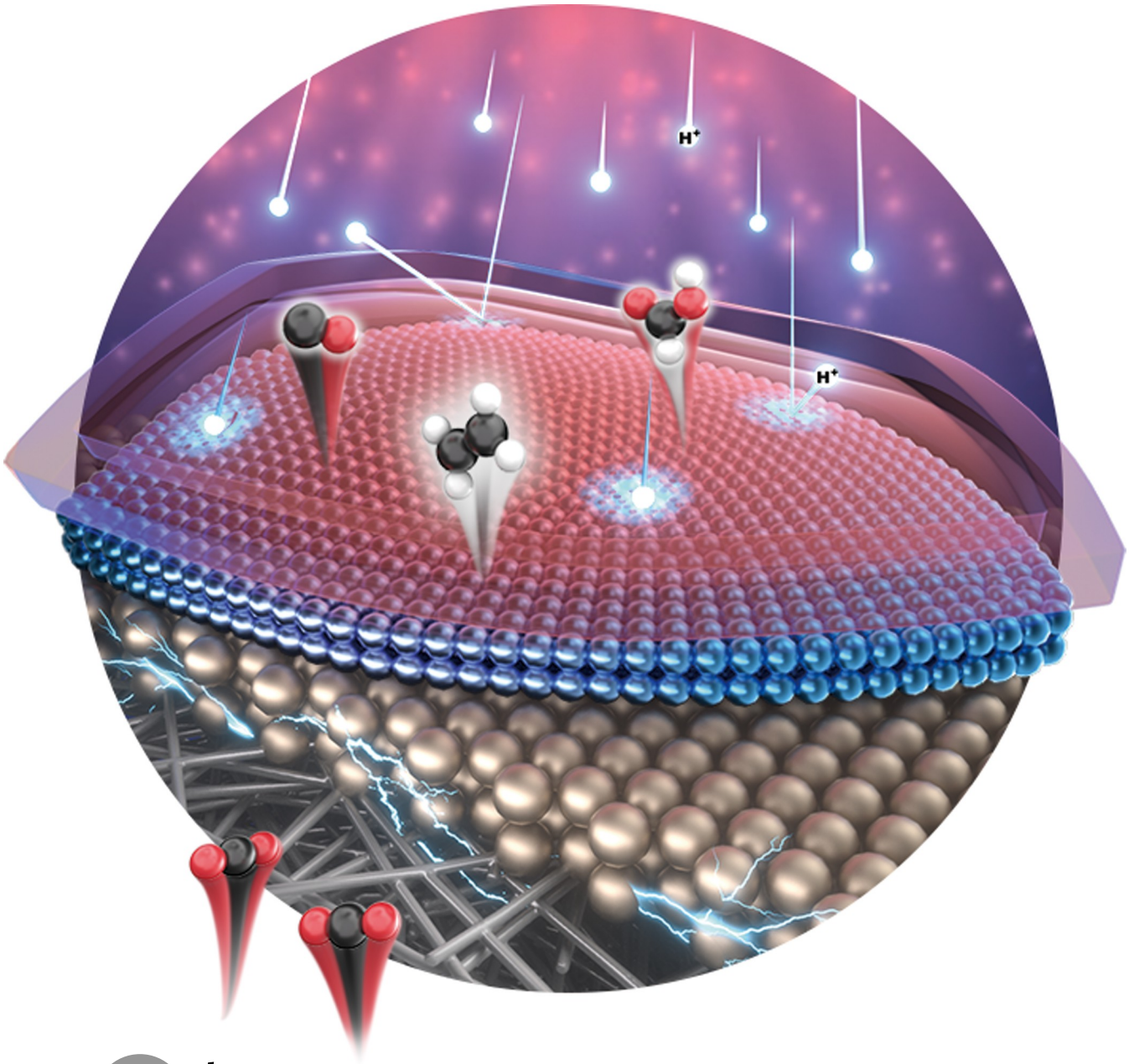

Abstract: Acidic CO_2 reduction (CO_2R) holds promise for the synthesis of low-carbon-footprint chemicals using renewable electricity. However, the corrosion of catalysts in strong acids causes severe hydrogen evolution and rapid deterioration of CO_2R performance. Here, by coating catalysts with an electrically nonconductive nanoporous SiC-Nafion™ layer, a near-neutral pH was stabilized on catalyst surfaces, thereby protecting the catalysts against corrosion for durable CO_2R in strong acids. Electrode microstructures played a critical role in regulating ion diffusion and stabilizing electrohydrodynamic flows near catalyst surfaces. This surface-coating strategy was applied to three catalysts, SnBi, Ag, and Cu, and they exhibited high activity over extended CO_2R operation in strong acids. Using a stratified SiC-Nafion™/SnBi/polytetrafluoroethylene (PTFE) electrode, constant production of formic acid was achieved with a single-pass carbon efficiency of $>75\,\%$ and Faradaic efficiency of $>90\,\%$ at $100\,mA\,cm^{-2}$ over 125 h at pH 1.

Introduction

Renewable-powered electrochemical CO_2 reduction (CO_2R) offers a promising strategy to address greenhouse gas CO_2 emissions and renewable chemical and fuel production.[1] Over the past few decades, significant effort has been devoted to improving the CO_2R activity and selectivity, particularly for converting CO_2 to carbon monoxide and formic acid, which show promising techno-economic feasibility for large-scale implementation.[2] Despite the highest CO_2R selectivity and productivity reported in alkaline electrolytes thus far, their low CO_2 utilization and the substantial consumption of hydroxide ions cause significant energy losses, limiting the viability of alkaline electrolyzers for practical long-term operation.[3]

In principle, CO_2 losses in acidic CO_2R are lesser than that of neutral and alkaline CO_2R electrolysis because carbonation formation is negligible in acidic electrolytes at $pH \leq 4$.[4] Theoretically, $\approx 100\,\%$ CO_2 utilization efficiency with near-zero carbonate crossover can be achieved in an acidic medium by recycling the unreacted CO_2 in the gas chamber and collecting liquid products, such as formic acid, from the cathodic stream. However, in strongly acidic electrolytes ($pH \leq 1$), the hydrogen evolution reaction (HER) competes with CO_2R and decreases the CO_2R Faradaic and energy efficiencies. Moreover, the operational stability of CO_2R catalysts in strong acids is compromised. Most CO_2R catalysts easily degrade with time in the harsh corrosive environments of strong acids.[3,4c] The most extended CO_2R stability reported thus far in strong acids is only limited to tens of hours.[3,4c] This lack of material and performance durability for long-term operation is a critical issue that must be overcome for the industrial application of acidic CO_2R technology.

The corrosion of electrocatalysts in strongly acidic environments is a significant concern in various applications, such as water splitting. As a result, several mitigation strategies have been developed, including doping electrocatalysts with noble metals or wrapping electrocatalysts with anticorrosive metal oxides,[5] carbides,[6] and nitrides.[7] However, these strategies are not directly applicable to CO_2R because first, doping with noble metals significantly alters the original electronic structures of the active sites of CO_2R electrocatalysts, promoting undesired HER.[8] Second, core/shell nanostructures limit CO_2 diffusion through the deposited surface shells to the core, leading to a considerable decrease in CO_2R activity.[9]

Herein, we propose an alternative approach based on the modification of the electrode structure. We show that by conformally coating the CO_2R catalysts with an electrically nonconductive ion-transport-regulating layer, the diffusion of cations and anions, particularly OH^- anions, was significantly suppressed within the nanostructures of the layer. As a result, a OH^--rich layer was maintained in direct contact with the catalyst surface during the reaction. This buried electrolyte/catalyst interface at a near-neutral pH created an inherently stable environment to protect the catalysts against corrosion at cathodic potentials during long-term CO_2R operation in strong acids. Moreover, the nanoporous characteristics of the coated layer further hindered the electrohydrodynamic flow of ions near the catalyst surfaces, resulting in a buildup of a high local concentration of potassium cations (K^+) and a near-neutral OH^- concentration within its structure. Consequently, improved CO_2R activity and durability with a reduced electrochemical ohmic loss were achieved.[3,4c,7,10] We applied this surface-coating strategy to three different catalysts for the durable production of formic acid, CO, and C_{2+} products over an extended CO_2R. Herein, using CO_2R-to-HCOOH conversion as an example, we report a combined performance benchmark of a high CO_2 single-pass carbon efficiency (SPCE) of 76 %, formic acid Faradaic efficiency (FE) of $>90\,\%$, and cathodic energy efficiency of 50 % at a commercially relevant current density of $100\,mA\,cm^{-2}$ over 125 h of continuous operation at pH 1.

Results and Discussion

Figure 1 compares the CO_2R processes in neutral-alkaline ($pH \geq 7$) and strongly acidic (pH 1) electrolytes and illustrates the effect of additional coating on the catalyst surface in an acidic medium. In this study, we mixed silicon carbide nanoparticles (SiC, Aladdin, ≈ 40 nm in diameter) with Nafion™ (Sigma–Aldrich, 5 %) to prepare SiC-Nafion™ inks that were later sprayed on the catalyst surface with different thicknesses. Because SiC and Nafion™ are electri-

[*] L. Li, Z. Liu, X. Yu, Prof. M. Zhong
College of Engineering and Applied Sciences, National Laboratory of Solid State Microstructures, Jiangsu Key Laboratory of Artificial Functional Materials, Nanjing University
163 Xianlin Avenue, Qixia District, Nanjing 210023 (China)
E-mail: miaozhong@nju.edu.cn

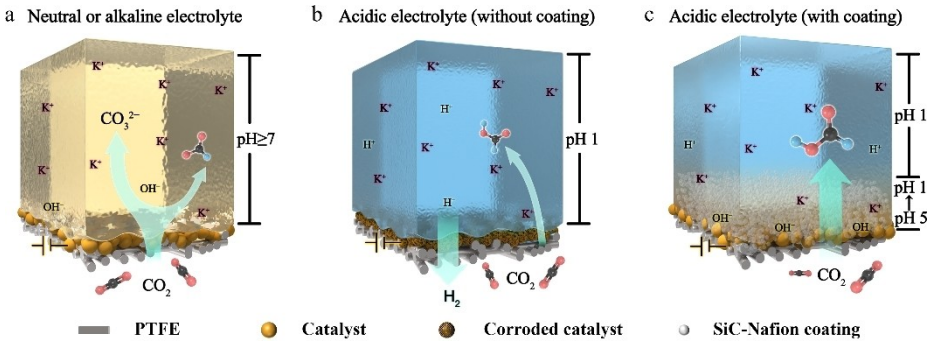

Figure 1. Schematic of electrochemical CO_2R in neutral-alkaline and acidic electrolytes with and without surface-coating layers. a) Production of formate and carbonate ions in neutral or alkaline CO_2R (pH $\geq$ 7), b) corrosion of the catalyst and parasitic HER during acidic CO_2R (pH 1), and c) application of the SiC-Nafrion™ coated layer and the resulting regulated pH and ion concentrations near the catalyst surface.

cally nonconductive and do not participate in electrochemical reactions, the intrinsic electrochemical properties of the underlying catalysts would be preserved. The compact SiC-Nafion™ coating also enables a favorable environment of a close-to-neutral pH with a high local K^+ concentration near the catalyst surfaces for CO_2R. The details will be discussed later.

The general effect of cations, such as K^+, on CO_2R, has been previously established. It has been shown that the presence of K^+ cations in the electrolyte increases the close-range electrostatic interactions that stabilize CO_2R intermediates. Moreover, K^+ slows the mass transport of H^+ to the catalyst surface.[11] Consequently, CO_2R dominates HER when high concentrations of K^+ are available. To further confirm these conjectures, we investigated the effect of K^+ concentration on the CO_2R and HER performances of three formic acid-selective catalysts. The catalyst fabrication is discussed in detail in Supporting Information. Linear sweep voltammetry (LSV) curves of SnBi, Bi, and Sn catalysts were recorded in 0.05 M H_2SO_4 and 3 M KCl electrolytes (pH 1) after the solutions were saturated with N_2 or CO_2 with a sweep speed of 10 mV s^{-1} in a flow cell. For all the catalysts, the onset potentials of CO_2R shift to more positive potentials (Figure 2a) in CO_2-saturated solutions compared to that of HER in N_2-saturated solutions. The HER activity is also suppressed (Figure S1). The SnBi catalyst shows the highest increase in CO_2R current densities (j_{CO2R}-j_{HER}) compared to Sn and Bi catalysts under identical operating conditions at pH 1 (Figure 2b). Additionally, density functional theory (DFT) studies reveal that in the presence of K^+ near the catalysts, the CO_2 to HCOOH conversion is promoted, and HER is suppressed (Figure 2c and Figures S4 and S5). In summary, an increase in the local K^+ concentration near the surfaces stabilized the *OCHO intermediate and weakened *H binding, thereby enhancing formic acid production over HER.

We subsequently explored the durability of the CO_2R performance of the SnBi catalyst in the CO_2-saturated

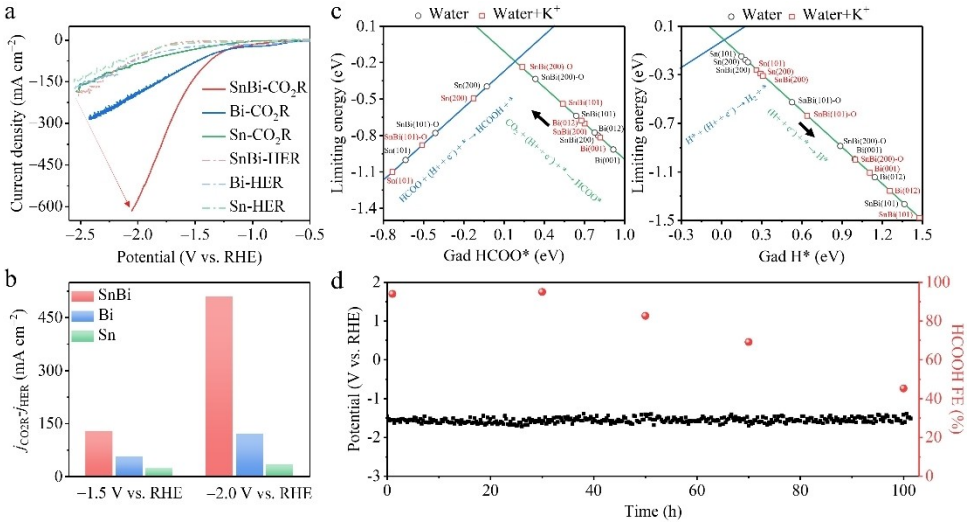

Figure 2. a) LSV curves of SnBi, Bi, and Sn catalysts in the 0.05 M H_2SO_4 and 3 M KCl electrolytes at pH 1 with CO_2 and N_2, respectively. b) Current densities (j_{CO2R}-j_{HER}) of SnBi, Bi, and Sn catalysts at −1.5 and −2.0 V_{RHE}. c) Reaction energy in the CO_2-to-HCOOH conversion and HER. d) FE of HCOOH for CO_2R using the SnBi catalyst without the SiC-Nafion™ coating in strong acid (pH = 1) at an applied current density of 100 mA cm^{-2}.

0.05 M H_2SO_2 and 3 M KCl electrolyte at pH 1. The FE of HCOOH dropped from 97% to 45% during 100 h of continuous operation at a constant current density of 100 mA cm^{-2} (Figure 2d). We then sprayed SnBi catalysts with various thicknesses (1–3 μm) of nanoporous SiC-Nafion™ to protect the electrocatalysts from corrosion (Figure 3a). We deposited SiC and Nafion™ mixtures (SiC, 10 wt%) in methanol on catalysts and dried the electrodes overnight to prepare nanoporous SiC-Nafion™ layers with the desired loading and thickness (Figures S6). We then inserted paper pH indicators (Merck, pH-measuring range: 0–14) between the nanoporous SiC-Nafion™ layers and underlying electrocatalysts and performed electrochemical CO_2R at a constant applied current density of 100 mA cm^{-2} in 0.05 M H_2SO_4 and 3 M KCl electrolyte for 20 min electrolysis. After the experiment, we carefully removed the surface nanoporous SiC-Nafion™ coating and determined the color change of the pH indicator. As shown in Figure 3b, the measured interface pH is higher when the thickness of the nanoporous SiC-Nafion™ is higher, indicating that coating the catalysts with nanoporous SiC-Nafion™ is effective in increasing the surface pH to close-to-neutral during CO_2R. Moreover, cross-sectional scanning electron microscopy (SEM) and energy dispersive X-ray spectroscopy (EDS) images of the post-reaction SiC-Nafion™/SnBi/polytetrafluoroethylene (PTFE) electrode reveal that K^+ is uniformly distributed in the nanoporous SiC-Nafion™ layer and on the catalyst surface (Figure 3d and 3e).

Furthermore, we constructed reaction and diffusion models in COMSOL Multiphysics® to simulate the pH profiles at the catalyst/SiC-Nafion™ interfaces during CO_2R using the conditions used for the experimental CO_2R (details are discussed in the Supporting Information and Figure S7). Our model shows that the pH at the catalyst/SiC-Nafion™ interfaces increases with an increase in the thickness of the SiC-Nafion™ layer (Figure 3c) at an applied current density of 100 mA cm^{-2}. With a 2 μm-thick SiC-Nafion™ coating, the simulated surface pH reached 4.5. This pH increase was due to the different diffusion coefficients of K^+ and OH^- and the large tortuosity of the nanoporous structure of the SiC-NafionTM layer that prolonged the diffusion distance of the ion. Once H^+ was consumed at the cathodic surface during CO_2R, the local OH^- near the surface was difficult to diffuse out of the surface-coated SiC-NafionTM nanostructures, thereby increasing the pH near the catalyst surface during the reaction. Moreover, the NafionTM in the SiC-Nafion™ layer allowed the transport of K^+ and retarded OH^- diffusion. As a result, a mildly neutral, K^+-rich layer was formed and maintained near the catalyst surface during the reaction. As shown by the electrochemical hydrodynamic simulations at pH 1 (Figure S8), the nanostructure also functions as a buffer layer to impede the flux of H^+ from the strongly acidic electrolyte bulk to the catalyst surface.[12] These results are in good agreement with the experimentally measured pH values at the catalyst/SiC-Nafion™ interface (Figure 3c), confirming the effective pH-regulating ability of the nanoporous SiC-Nafion™.

To further understand the role of the surface pH on the composition and structural changes of the electrocatalysts during CO_2R, we performed SEM, high-resolution transmission electron microscopy (HRTEM), and scanning transmission electron microscopy (STEM)-EDS measurements on the post-reaction SnBi catalysts with and without a 3 μm-thick SiC-Nafion™ coating. The CO_2R reaction was conducted for different time courses at 100 mA cm^{-2} in the 0.05 M H_2SO_4 and 3 M KCl electrolyte at pH 1. As shown in Figure 4a and 4b and Figure S9a, without the SiC-Nafion™ coating, the morphology of the catalyst is mostly preserved; however, a layer of small SnO_2 nanoparticles is observed on

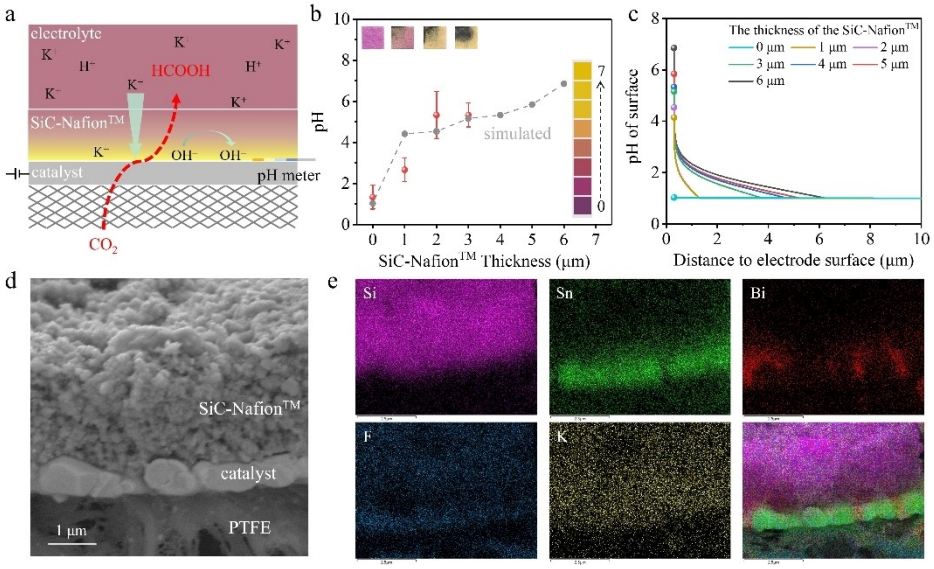

Figure 3. Surface pH of the SnBi and SiC-Nafion™-coated SnBi electrocatalysts. a) Schematic of catalysts during CO_2R at pH 1. b) Surface pH vs. SiC-Nafion™ layer thickness. c) Simulations of the pH distribution from the catalyst surface to the electrolyte bulk with different thicknesses of SiC-Nafion™ coatings. d) Cross-section SEM image of SiC-Nafion™/SnBi/PTFE. e) Cross-section SEM-EDS analyses of SiC-Nafion™/SnBi/PTFE.

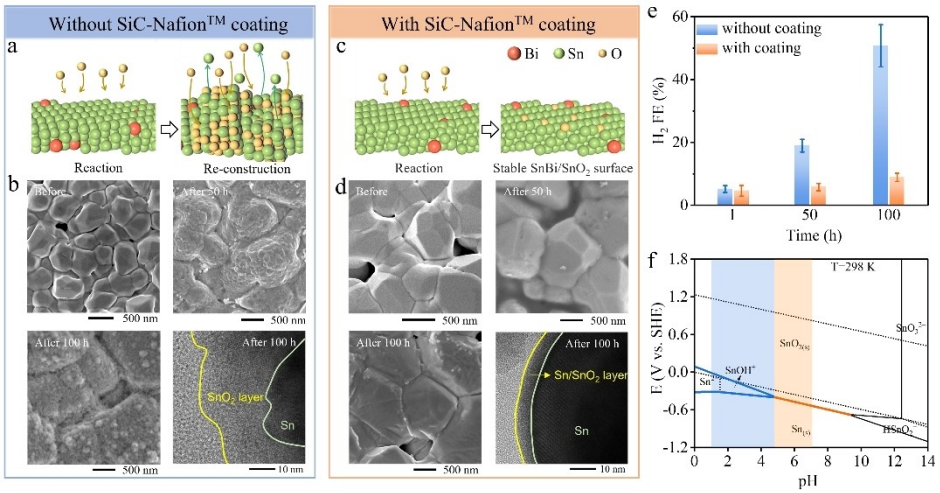

Figure 4. Structural analyses of the SnBi and SiC-Nafion™-coated SnBi electrocatalysts. a) Schematic of a proposed regrowth process at pH 1, whereby the simultaneous dissolution and redeposition of Sn^{2+}, $SnOH^{+}$, and SnO_2 lead to a structural change. b) SEM and TEM images of SnBi catalysts before and after 50 and 100 h reactions in a 0.05 M H_2SO_4 and 3 M KCl electrolyte. c) schematic of a proposed passivation process at pH 4.5–8, whereby an immobilized solid/solid Sn/SnO_2 surface is formed. d) SEM and TEM images of SnBi catalysts before and after 50 and 100 h reaction in a 0.05 M H_2SO_4 and 3 M KCl electrolyte with a 3 μm SiC-Nafion™ coating. e) FE of H_2 for SnBi catalysts with and without SiC-Nafion™ coating at 100 mA cm^{-2} throughout a 100 h CO_2R. f) Pourbaix diagram of Sn.

the catalyst surface after 50 and 100 h of CO_2R. Based on the TEM images and STEM-EDX analyses (Figure 4b and Figure S10), the thickness of the grown SnO_2 layer is 20–30 nm. This thick layer essentially alters the catalytically active sites on the catalyst surface and significantly promotes HER, as confirmed by H_2 FE of ≈50 % obtained after 100 h of CO_2R in the absence of the SiC-Nafion™ coating (Figure 4e). The TEM analysis of the surface of the SnBi catalysts with a significantly thin SiC-Nafion™ coating (3 μm) after 50 and 100 h of CO_2R also does not indicate any significant morphology changes (Figure 4c and 4d and Figure S9b), and TEM and STEM-EDX analyses reveal the formation of a uniform and significantly thin (≈5 nm) Sn/SnO_2 layer on the SnBi catalysts (Figure S11). Contrary to the thicker SnO_2 layers, thinner Sn/SnO_2 layers formed stable and active $SnBi/SnO_2$ surfaces that efficiently retained the CO_2R activity and suppressed the H_2 FE to below 10 % during the 100-h reaction.

Based on these findings, we propose a catalyst corrosion and regrowth model and a catalyst passivation model for SnBi electrocatalysts at surface pH values of 1 and 4.5–9, respectively. We speculate that because the potentials measured on the catalyst surfaces may fluctuate during CO_2R, random chemical oxidation may occasionally occur. As shown in the Pourbaix image of Sn in Figure 4f, metallic Sn could be oxidized to yield soluble Sn^{2+} and $SnOH^{+}$ species at pH 1 when the potentials unexpectedly changed to oxidative values. These soluble Sn^{2+} and $SnOH^{+}$ species could be reduced back to Sn^0 when reductive conditions were presumed (catalyst regrowth).[13] This back-and-forth dissolution and redeposition of Sn^{2+} and $SnOH^{+}$ on the catalyst surfaces during the long-term CO_2R could have detrimental effects on the catalyst activity. Based on the Sn Pourbaix diagram (Figure 4f), at pH values 4.5–9, SnO_2 is the dominant species, and no dissolved Sn^{2+} or $SnOH^{+}$ are expected, explaining the formation of an immobilized Sn/SnO_2 solid/solid layer. Dissolution and regrowth did not occur. Instead, the redox modulation[14] between Sn and SnO_2 on the immobilized surface can promote the catalyst stability and retain the high CO_2R activity during the extended reaction, as observed with the 3 μm SiC-Nafion™-coated SnBi catalysts during 100 h of CO_2R.

Next, the CO_2R activity of the SiC-Nafion™/SnBi/PTFE electrodes was studied in flow cells. We also performed CO_2R using SiC-Nafion™/Sn/PTFE and SiC-Nafion™/Bi/PTFE catalysts under conditions identical to that of the CO_2R of SiC-Nafion™/SnBi/PTFE for comparison. The FEs of liquid and gaseous products were calculated using ion chromatography (IC) and gas chromatography (GC) data, respectively. Figure 5a shows the FE values of HCOOH and H_2 obtained with the SiC-Nafion™-coated Bi, Sn, and SnBi catalysts across a wide range of current densities. The SiC-Nafion™/SnBi/PTFE catalysts exhibit stable HCOOH FEs (>92 %) with limited H_2 production at 100–800 mA cm^{-2}, indicating its high selectivity for electrochemical CO_2-to-HCOOH conversion, consistent with the LSV experimental results (Figure 2a). Based on these results, a cathode energy efficiency (CEE) for the production of HCOOH of 50 % is obtained with SiC-Nafion™/SnBi/PTFE in the flow cell at 100 mA cm^{-2} (Figure 5a). Figure S12 depicts the HCOOH production SPCE using the SiC-Nafion™/SnBi/PTFE catalyst at different pH values as a function of the CO_2 flow rate (3, 6, and 10 sccm). In a single flow cell with an active area of 1.7 cm ×1.7 cm, an SPCE of 65 % was achieved for HCOOH at a CO_2 flow rate of 3 sccm and current density of 100 mA cm^{-2}. Considering the low amounts of H_2 generated at 100 mA cm^{-2} (H_2 FE < 10 %), the CO_2 concentration at the outlet of the gas chamber was not influenced by H_2. We then performed CO_2R in a tandem system comprising two flow cells connected in series (1.7 cm ×1.7 cm each). A

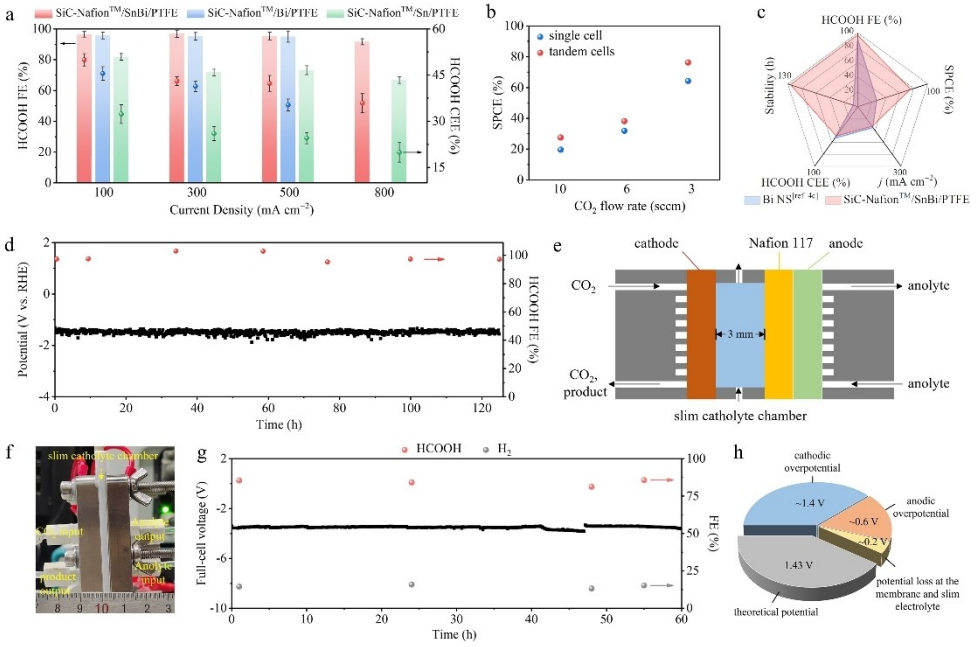

Figure 5. CO_2R performance on SiC-Nafion™/SnBi/PTFE, SiC-Nafion™/Sn/PTFE, and SiC-Nafion™/Bi/PTFE in the 0.05 M H_2SO_4 with 3 M KCl electrolyte at pH 1. a) FEs and half-cell energy efficiencies (CEEs) for HCOOH production with three catalysts at different current densities from 100–800 mA cm^{-2}. b) SPCE of CO_2R-to-HCOOH with SiC-Nafion™/SnBi/PTFE catalysts at 100 mA cm^{-2} at different CO_2 flow rates. c) Comparison of CO_2R-to-HCOOH SPCE, FE, CEE, current density, and stability of the as-developed and previously reported materials under acidic conditions. d) CO_2R chronopotentiometry curve with the HCOOH FE at 100 mA cm^{-2} in a 0.05 M H_2SO_4 and 3 M KCl electrolyte at pH 1. (e, f) Schematic and optical image of a slim-catholyte MEA. (g) CO_2R performance of a SiC-Nafion™/SnBi/Cu/PTFE electrode in a slim-catholyte MEA device at a current density of 100 mA cm^{-2} without *i*R compensation. (h) The overpotential losses on each part in an MEA cell.

significant SPCE of 76 % is achieved at a 3 sccm CO_2 flow rate and a current density of 100 mA cm^{-2}, implying that >75 % of the gaseous CO_2 is converted to HCOOH (Figure 5b).

Notably, the SiC-Nafion™/SnBi/PTFE electrode maintains a stable operational voltage (−1.5 V_{RHE}) and HCOOH FE (95 %) over 125 h of continuous CO_2R operation in a strong acid at pH 1 (Figure 5d). We concluded that this outstanding CO_2R performance in strong acid was due to the SiC-Nafion™ surface-coating treatment, which effectively increased the local pH, establishing a stable solid/solid interface to prolong the operating lifetime of the catalyst and CO_2R-to-HCOOH production.

We also present the benchmark performance of SiC-Nafion™/SnBi/PTFE by comparing it to that of the previously reported acidic CO_2R results (Figure 5c). Considering the high formic acid selectivity at high current densities, high carbon efficiency, and long-term stability, SiC-Nafion™/SnBi/PTFE reported herein clearly outperforms the previously reported catalysts without surface coating.[4c] We also compared the CO_2R performances of Ag and Cu catalysts with and without the SiC-Nafion™ coating in the same 0.05 M H_2SO_4 and 3 M KCl electrolyte at pH = 1 (Figures S13–S15) to further demonstrate the viability of the developed surface-coating strategy. Significantly, the morphologies and performance of Ag and Cu are retained with the 3 μm SiC-Nafion™ coating after 50 h of CO_2R operation, whereas corrosion occurs with the catalysts that are not coated with the SiC-Nafion™ layer (Figures S16 and S17). Therefore, surface-coating with SiC-Nafion™ is a unique and effective strategy for protecting catalysts from reconstruction and significantly improves the CO_2R stability in acids for the selective production of formate, CO, and ethylene.

To validate the effectiveness of the SiC-Nafion™ approach in a practical cell setup, we conducted acidic CO_2R experiments for SiC-Nafion™/SnBi/Cu/PTFE and SiC-Nafion™/Cu/PTFE in both zero-gap and slim-catholyte-chamber (3 mm) MEA-based electrolyzers at pH 1 (Figure 5e, 5f). Using a stratified, electrically conductive SiC-Nafion™/SnBi/Cu/PTFE electrode, we achieved a continuous, nearly 90 % HCOOH FE over 60 hours at 100 mA cm^{-2} in a slim-catholyte MEA cell (Figure 5g and Figure S18). Our analysis of the potential loss in each part of the MEA is presented in Figure S19 and Figure 5h, indicating that reducing the overpotentials on the anodes and cathodes remains the current limitation in acidic CO_2R. Further, we applied the same electrode design to the SiC-Nafion™/Cu/PTFE electrode, leading to the improved performance of 45 % C_2H_4 FE in the slim-catholyte MEA devices over 30 hours (Figure S20).

Finally, we used the high-performance SiC-Nafion™/SnBi/PTFE catalyst in a solid-state CO_2R electrolyzer to produce pure formic acid (Figure S21).[15] As shown in Figure S22, the FE of HCOOH reaches 91.8 % at a high current density of 150 mA cm^{-2} and a modest full-cell potential of ≈4.45 V at room temperature. The solid-state CO_2R electrolyzer study indicated that further reduction of

the electrical resistance in the thick proton transfer layer is beneficial for enhancing performance. After 12 h of continuous operation, a 0.41 M solution of pure HCOOH is produced with an FE of 82 % (Figure S23)

Conclusion

In summary, we developed an effective strategy to improve the prolonged CO_2R performance in highly acidic media. We demonstrated that by coating the catalyst layer with an electrically nonconductive nanoporous ion-regulatory layer, efficient, selective, and stable CO_2R could be conducted at pH 1. We elucidated that the surface pH and local K^+ accumulation were the key contributors to the stabilization of the high CO_2R performance and durability of the electrocatalysts during long-term operation. We also demonstrated that the developed surface-coating strategy was universal for improving the CO_2R performance and stability of the most common metallic CO_2R catalysts (SnBi, Ag, and Cu) in strong acids. This electrode structure engineering strategy will provide a useful pathway for achieving an HER-free, efficient, and stable CO_2R with high CO_2 utilization for low-temperature CO_2 electrolysis in acidic media.

Experimental Section

Experimental Details are provided in Supporting Information.

Acknowledgements

This work was financially supported by the National Key R&D Program of China (No. 2020YFA0406102), the National Natural Science Foundation of China (grant numbers 22272078 and 91963121), the Frontiers Science Center for Critical Earth Material Cycling of Nanjing University, and the "Innovation and Entrepreneurship of Talents plan" of Jiangsu Province.

Conflict of Interest

The authors declare no conflict of interest.

Data Availability Statement

The data that support the findings of this study are available from the corresponding author upon reasonable request.

Keywords: Acidic Electrocatalysis · CO_2 Reduction · Carbon Conversion Efficiency · Electrochemistry · Surface Chemistry

[1] a) M. He, Y. Sun, B. Han, *Angew. Chem. Int. Ed.* **2022**, *61*, e202112835; *Angew. Chem.* **2022**, *134*, e202112835; b) O. S. Bushuyev, P. De Luna, C. T. Dinh, L. Tao, G. Saur, J. van de Lagemaat, S. O. Kelley, E. H. Sargent, *Joule* **2018**, *2*, 825–832; c) D. Grammatico, A. J. Bagnall, L. Riccardi, M. Fontecave, B. L. Su, L. Billlon, *Angew. Chem. Int. Ed.* **2022**, *61*, e202206399; *Angew. Chem.* **2022**, *134*, e202206399; d) A. Ozden, F. P. García de Arquer, J. E. Huang, J. Wicks, J. Sisler, R. K. Miao, C. P. O'Brien, G. Lee, X. Wang, A. H. Ip, E. H. Sargent, D. Sinton, *Nat. Sustainability* **2022**, *5*, 563–573; e) M. Zhong, K. Tran, Y. Min, C. Wang, Z. Wang, C. T. Dinh, P. De Luna, Z. Yu, A. S. Rasouli, P. Brodersen, S. Sun, O. Voznyy, C. S. Tan, M. Askerka, F. Che, M. Liu, A. Seifitokaldani, Y. Pang, S. C. Lo, A. Ip, Z. Ulissi, E. H. Sargent, *Nature* **2020**, *581*, 178–183.

[2] a) M. G. Kibria, J. P. Edwards, C. M. Gabardo, C. T. Dinh, A. Seifitokaldani, D. Sinton, E. H. Sargent, *Adv. Mater.* **2019**, *31*, 1807166; b) M. Jouny, W. Luc, F. Jiao, *Ind. Eng. Chem. Res.* **2018**, *57*, 2165–2177; c) C. Chen, J. F. Khosrowabadi Kotyk, S. W. Sheehan, *Chem* **2018**, *4*, 2571–2586; d) T. Zheng, C. Liu, C. Guo, M. Zhang, X. Li, Q. Jiang, W. Xue, H. Li, A. Li, C. W. Pao, J. Xiao, C. Xia, J. Zeng, *Nat. Nanotechnol.* **2021**, *16*, 1386–1393.

[3] J. E. Huang, *Science* **2021**, *372*, 1074–1078.

[4] a) M. Oßkopp, A. Löwe, C. M. S. Lobo, S. Baranyai, T. Khoza, M. Auinger, E. Klemm, *J. CO2 Util.* **2022**, *56*, 101823; b) J. A. Rabinowitz, M. W. Kanan, *Nat. Commun.* **2020**, *11*, 5231; c) Y. Qiao, W. Lai, K. Huang, T. Yu, Q. Wang, L. Gao, Z. Yang, Z. Ma, T. Sun, M. Liu, C. Lian, H. Huang, *ACS Catal.* **2022**, *12*, 2357–2364.

[5] Y. J. Tang, M. R. Gao, C. H. Liu, S. L. Li, H. L. Jiang, Y. Q. Lan, M. Han, S. H. Yu, *Angew. Chem. Int. Ed.* **2015**, *54*, 12928–12932; *Angew. Chem.* **2015**, *127*, 13120–13124.

[6] X. Fan, Z. Peng, R. Ye, H. Zhou, X. Guo, *ACS Nano* **2015**, *9*, 7407–7418.

[7] X. Dai, Z. Li, Y. Ma, M. Liu, K. Du, H. Su, H. Zhuo, L. Yu, H. Sun, X. Zhang, *ACS Appl. Mater. Interfaces* **2016**, *8*, 6439–6448.

[8] X. Liu, J. Xiao, H. Peng, X. Hong, K. Chan, J. K. Norskov, *Nat. Commun.* **2017**, *8*, 15438.

[9] C. Zhu, L. Zhou, Z. Zhang, C. Yang, G. Shi, S. Zhao, H. Gu, J. Wu, X. Gao, Y. Li, K. Liu, S. Dai, L. Zhang, *Chem* **2022**, *8*, 3288–3301.

[10] J. Gu, S. Liu, W. Ni, W. Ren, S. Haussener, X. Hu, *Nat. Catal.* **2022**, *5*, 268–276.

[11] M. C. O. Monteiro, F. Dattila, B. Hagedoorn, R. García-Muelas, N. López, M. T. M. Koper, *Nat. Catal.* **2021**, *4*, 654–662.

[12] E. Karatay, C. L. Druzgalski, A. Mani, *J. Colloid Interface Sci.* **2015**, *446*, 67–76.

[13] P. De Luna, R. Quintero-Bermudez, C.-T. Dinh, M. B. Ross, O. S. Bushuyev, P. Todorović, T. Regier, S. O. Kelley, P. Yang, E. H. Sargent, *Nat. Catal.* **2018**, *1*, 103–110.

[14] L. Li, A. Ozden, S. Guo, A. D. A. F. P. Garci, C. Wang, M. Zhang, J. Zhang, H. Jiang, W. Wang, H. Dong, D. Sinton, E. H. Sargent, M. Zhong, *Nat. Commun.* **2021**, *12*, 5223.

[15] H. Yang, J. J. Kaczur, S. D. Sajjad, R. I. Masel, *J. CO2 Util.* **2017**, *20*, 208–217.

Manuscript received: January 5, 2023
Accepted manuscript online: February 21, 2023
Version of record online: March 8, 2023